Available online at www.sciencedirect.com
SCIENCE DIRECT®
Journal of Sound and Vibration 280 (2005) 181–209
JOURNAL OF SOUND AND VIBRATION
www.elsevier.com/locate/jsvi

The radiation efficiency of baffled plates and strips

G. Xie, D.J. Thompson*, C.J.C. Jones

Institute of Sound and Vibration Research, University of Southampton, Highfield, Southampton SO17 1BJ, UK

Received 11 March 2003; accepted 4 December 2003

Abstract

The average radiation efficiency of point-excited rectangular plates, including those with a very large aspect ratio ('strips'), is investigated by using a modal summation method based on the farfield sound intensity. By taking an average over all possible forcing positions on the plate, the cross-modal contributions average out to zero. The numerical results from the modal summation are compared with established formulae for rectangular plates. For wavenumbers where acoustic circulation takes place, it is shown that the previously published formulae are not applicable for predicting the average radiation efficiency for a strip. The analysis for the strip reveals that the radiation efficiency at frequencies below the first structural natural frequency of the strip is proportional to the square of the shortest edge length. At frequencies between the fundamental natural frequency and that of the second order mode of bending across the strip, the average radiation efficiency is found to be proportional to the structural damping loss factor, but differs from the results obtained from the usual model of the nearfield radiation from the forcing point of a rectangular plate. Approximate expressions for calculating the average radiation efficiency of the strip are derived. The maximum radiation efficiency around the critical frequency is found to vary less with Helmholtz number $k_c a$, where k_c is the wavenumber at the critical frequency and a is the width, than previously published models suggest.

1. Introduction

The sound radiation from a vibrating rectangular plate is of great practical importance and has been investigated extensively over many years. For a flat plate set in an infinite baffle, the radiated sound field can be calculated by a Rayleigh integral approach [1]. There are two common approaches used to determine the radiation efficiency, or resistance, theoretically. The first is to integrate the farfield acoustic intensity over a hemisphere enclosing the plate. The other approach is to integrate the acoustic intensity over the surface of the vibrating plate. Both approaches

*Corresponding author. Tel.: +44-23-8059-2510; fax: +44-23-8059-3190.
E-mail address: djt@isvr.soton.ac.uk (D.J. Thompson).

0022-460X/$ - see front matter © 2004 Elsevier Ltd. All rights reserved.
doi:10.1016/j.jsv.2003.12.025

require a knowledge of the distribution of vibration velocity over the plate. This is usually obtained by assuming the boundary conditions are simple supports. Since plate vibrations generally involve many superimposed modes, the radiation efficiency of a plate, in principle, can be obtained by summing the effect of all the modes that contribute significantly in the frequency range under consideration.

The radiation efficiency of a single mode of the plate is usually called the modal radiation efficiency. The total radiation efficiency of the plate is called either the 'average radiation efficiency' or the 'weighted radiation efficiency'. In the literature, both the terms 'radiation resistance' and 'radiation efficiency' are used, the latter being the radiation resistance normalized by the surface area and the impedance of air. The radiation efficiency is thus defined by

$$\sigma = \frac{R_{rad}}{\rho c S} = \frac{W_{rad}}{\rho c S \langle \overline{v^2} \rangle}, \tag{1}$$

where R_{rad} is radiation resistance, W_{rad} is power radiated by the plate, S is the area of the plate, $\langle \overline{v^2} \rangle$ is the spatially averaged mean square velocity of the plate, ρ and c are the density of air and the speed of sound in air.

For a detailed study of the radiation it is necessary to derive expressions for the radiation resistance of particular structural mode shapes of the plate. As early as the 1960s, Maidanik [2] first proposed several approximate formulae for calculating the modal radiation resistance in the whole frequency range. Wallace [3] presented integral expressions for the modal radiation efficiency of rectangular plates at arbitrary frequencies based on farfield acoustic intensity. Approximate expressions of radiation efficiencies for frequencies well below the critical frequency were also presented. He investigated the effects on radiation efficiency of the inter-nodal areas and their aspect ratios. The characteristics of the radiation from a baffled rectangular plate were clearly shown. Gomperts [4,5] investigated the modal radiation of a rectangular plate under general boundary conditions. It was found by Gomperts that plates with greater edge-constraints do not always have larger radiation efficiencies than less edge-constrained ones, and the radiation efficiencies for two-dimensional vibration patterns differ rather considerably from those for one-dimensional vibration patterns.

In addition to these methods, Heckl [6] analyzed sound radiation of planar sources by using a Fourier transform approach in k-space (wavenumber space). Leppington [7] later introduced several asymptotic formulae to calculate the modal radiation efficiency for large acoustic wavenumbers, especially in the range close to the critical frequency. Williams [8] proposed a series expansion in ascending powers of the wavenumber k for the acoustic power radiated from a planar source. Most recently, Li [9] gave an analytical solution, in the form of a power series of the non-dimensional acoustic wavenumber, to calculate the modal radiation resistance of a rectangular plate for moderate wavenumbers.

As well as modal radiation resistances, the average radiation of a plate has also been an active subject of study because of its practical importance. It was also Maidanik [2] who first applied the concept of power flow and statistical energy analysis to overcome the burdensome calculation at higher frequencies where many modes contribute to the vibration of a plate. He presented a formula for the average radiation resistance based on the assumption of a reverberant vibration field (equal modal energy). A similar modal-average radiation curve was presented in Ref. [10]. Leppington [7] re-investigated the problem of average radiation efficiency and revised some of

Maidanik's work, using the assumption of high modal densities for the plate. His assumption is based on the same principle as Maidanik's. It was found in Leppington's study that Maidanik overestimated the radiation resistance at coincidence, particularly for a plate with a very large aspect ratio. Leppington also gave an equivalent formula to Maidanik's for large acoustic wavenumbers.

However, in the works of both Maidanik and Leppington, the radiation resistance was considered without including the cross-mode contributions. Snyder and Tanaka [11] introduced the contribution of the cross-modal couplings to calculate the total acoustic power at low frequency using modal radiation efficiencies. It was shown that the cross-mode contributions are only non-zero for pairs of modes that are either both odd or both even in a given direction. The mutual radiation resistance was also investigated recently by Li and Gibeling [12,13]. It was found that the cross-modal coupling could have a significant impact on the radiated power, even at a resonance frequency. The cross-modal contributions were also included in the power series of Li [9].

Although the 'strips' considered in this paper are no more than rectangular plates of large aspect ratio, it will be shown that, for a certain frequency range, the classic formulae previously obtained for the rectangular plate are not suitable. Sakagami and Michishita [14,15] investigated the characteristic of the sound field radiated by a baffled and unbaffled strip with infinite length under different excitation. However, only the sound pressure for certain given positions was studied and the radiation efficiency of the strips was not presented.

Here, the average radiation efficiency of a point-excited rectangular plate is considered first in terms of the summation of its normal modes. Using an average over force point locations it is shown that the cross-modal coupling averages to zero. The average radiation efficiency of a strip is then investigated numerically using the method. Approximate formulae, applicable at frequencies below the critical frequency, are developed and compared with the numerical results, and the maximum radiation efficiency around the critical frequency is also analyzed.

2. Derivation of average radiation efficiency using a modal summation approach

2.1. Radiated power in terms of plate modes

Consider a rectangular plate, simply supported on four edges and set in an infinite rigid baffle as shown in Fig. 1. For harmonic motion at frequency ω, the total acoustic power radiated from the plate can be obtained by integrating the farfield acoustic intensity over a hemisphere of radius r to give

$$W = \int_0^{2\pi} \int_0^{\pi/2} \frac{|p(\mathbf{r})|^2}{2\rho c} r^2 \sin\theta \, \mathrm{d}\theta \, \mathrm{d}\phi, \tag{2}$$

where $p(\mathbf{r})$ is the complex acoustic pressure amplitude at a location in space expressed in spherical co-ordinates, $\mathbf{r} = (r, \theta, \phi)$ at frequency ω.

The complex acoustic pressure amplitude $p(\mathbf{r})$ can be written in terms of the plate surface velocity using the Rayleigh integral [1],

$$p(\mathbf{r}) = \frac{\mathrm{j}k\rho c}{2\pi} \int_s v(\mathbf{x}) \frac{\mathrm{e}^{-\mathrm{j}kr'}}{r'} \mathrm{d}\mathbf{x}, \tag{3}$$

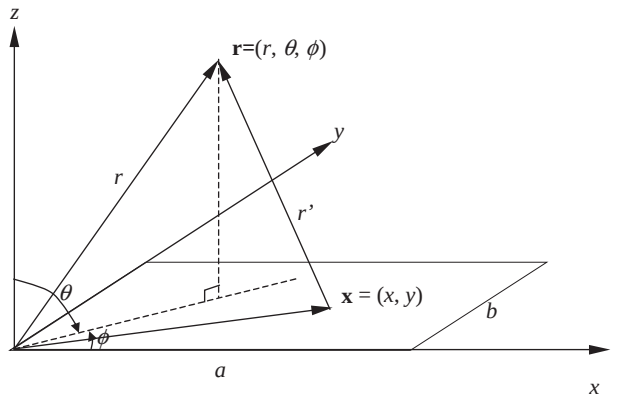

Fig. 1. Co-ordinate system of a vibrating rectangular plate.

where $v(\mathbf{x})$ is the complex surface normal velocity amplitude at location $\mathbf{x} = (x, y)$, $k = \omega/c$ is the acoustic wavenumber and the integral is evaluated over the plate surface S. The distance $r' = |\mathbf{r} - \mathbf{x}|$.

The velocity $v(\mathbf{x})$ at any location $\mathbf{x}$ on the structure can be found by superposing the modal contributions from each mode of structural vibration of the plate as

$$v(\mathbf{x}) = \sum_{m=1}^{\infty} \sum_{n=1}^{\infty} u_{mn} \varphi_{mn}(\mathbf{x}), \tag{4}$$

where u_{mn} is the complex velocity amplitude of the mode (m, n), $\varphi_{mn}(\mathbf{x})$ is the value of the associated mode shape function at the location $\mathbf{x}$, and m, n are the indices of the modes. u_{mn} depends on the form of the excitation and on frequency. The mode shape function $\varphi_{mn}(\mathbf{x})$ for the simply supported rectangular plate can be expressed as

$$\varphi_{mn}(x, y) = \sin\left(\frac{m\pi x}{a}\right) \sin\left(\frac{n\pi y}{b}\right). \tag{5}$$

Substituting Eqs. (4) and (5) into Eq. (3), and rearranging the order of summation and integral, the sound pressure is given by

$$p(\mathbf{r}) = \sum_{m=1}^{\infty} \sum_{n=1}^{\infty} u_{mn} \left\{ \frac{\mathrm{j}k\rho c}{2\pi} \int_s \varphi_{mn}(\mathbf{x}) \frac{\mathrm{e}^{-\mathrm{j}kr'}}{r'} \mathrm{d}\mathbf{x} \right\} = \sum_{m=1}^{\infty} \sum_{n=1}^{\infty} u_{mn} A_{mn}(\mathbf{r}). \tag{6}$$

From Wallace [3], the term in the brackets, called $A_{mn}(\mathbf{r})$ here, is given by

$$A_{mn}(\mathbf{r}) = jk\rho c \frac{\mathrm{e}^{-\mathrm{j}kr}}{2\pi r} \frac{ab}{\pi^2 mn} \left[\frac{(-1)^m \mathrm{e}^{\mathrm{j}\alpha} - 1}{(\alpha/(m\pi))^2 - 1} \right] \left[\frac{(-1)^n \mathrm{e}^{\mathrm{j}\beta} - 1}{(\beta/(n\pi))^2 - 1} \right], \tag{7}$$

where $\alpha = ka \sin\theta \cos\phi$ and $\beta = kb \sin\theta \sin\phi$, and $r = |\mathbf{r}|$.

The substitution of Eq. (6) into Eq. (2) gives the total radiated power of the plate as

$$W = \sum_{m=1}^{\infty}\sum_{n=1}^{\infty}\sum_{m'=1}^{\infty}\sum_{n'=1}^{\infty}\left\{u_{mn}u_{m'n'}^{*}\int_{0}^{2\pi}\int_{0}^{\pi/2}\frac{A_{mn}(\mathbf{r})A_{m'n'}^{*}(\mathbf{r})}{2\rho c}r^{2}\sin\theta\,\mathrm{d}\theta\,\mathrm{d}\phi\right\}, \tag{8}$$

where m' and n' are used to distinguish m and n in the conjugate. From this equation, it can be seen that the total radiated power depends on the contribution of combinations of modes. The contribution is usually referred to as the self-modal radiation for $m = m'$ and $n = n'$, and cross-modal radiation for either $m \neq m'$ or $n \neq n'$.

Eq. (8) can also be expressed in a matrix form,

$$W = \mathbf{u}^{\mathrm{T}}\mathbf{D}\mathbf{u}, \tag{9}$$

where $\mathbf{u}$ is a column vector of terms u_{mn} and $\mathbf{D}$ is a matrix of integral terms. The diagonal elements of $\mathbf{D}$ are the self-modal terms and the off-diagonal elements are the mutual radiation terms. According to Snyder and Tanaka [11], cross-modal radiation only occurs between a pair of modes with a similar index-type (i.e., either both odd or both even in each direction). Hence, many off-diagonal terms are zero and only a quarter of the matrix elements are non-zero.

It is clear that the calculation of total radiation efficiency requires the calculation of both self- and cross-modal radiation terms described in Eq. (8). At the same time, a knowledge of the excitation is also required to determine $\mathbf{u}$.

2.2. Response to point force

Consider a point force applied on the plate at location (x_0, y_0). The modal velocity amplitude is given by [16]

$$u_{mn} = \frac{\mathrm{j}\omega F\varphi_{mn}(x_0, y_0)}{[\omega_{mn}^{2}(1+\mathrm{j}\eta)-\omega^{2}]M_{mn}}, \tag{10}$$

where F is the force amplitude, ω_{mn} is the natural frequency, η is the damping loss factor, assuming hysteretic damping, and M_{mn} is the modal mass that is given by

$$M_{mn} = \int_{S}\rho_s h\varphi_{mn}^{2}(x,y)\,\mathrm{d}S = \tfrac{1}{4}\rho_s hab = \frac{M}{4}, \tag{11}$$

where ρ_s and h are the density and thickness of the plate, M is the mass the plate and use is made of the form of φ_{mn} from Eq. (5). The natural frequencies ω_{mn} are given by

$$\omega_{mn} = \left(\frac{B}{\rho_s h}\right)^{1/2}\left[\left(\frac{m\pi}{a}\right)^{2}+\left(\frac{n\pi}{b}\right)^{2}\right], \tag{12}$$

where B is the bending stiffness of the plate.

2.3. Average over forcing points

For the purpose of obtaining a general result for the total radiated power, the average of all possible locations of the uncorrelated point forces on the plate is considered. This averaged

radiated power can be written as

$$\bar{W} = \frac{1}{ab}\int_0^a \int_0^b W \,\mathrm{d}x_0 \,\mathrm{d}y_0$$

$$= \sum_{m=1}^{\infty}\sum_{n=1}^{\infty}\sum_{m'=1}^{\infty}\sum_{n'=1}^{\infty}\left\{\frac{1}{ab}\int_0^a \int_0^b u_{mn}u_{m'n'}^* \,\mathrm{d}x_0 \,\mathrm{d}y_0 \int_0^{2\pi}\int_0^{\pi/2} \frac{A_{mn}(\mathbf{r})A_{m'n'}^*(\mathbf{r})}{2\rho c} r^2 \sin\theta \,\mathrm{d}\theta \,\mathrm{d}\phi\right\}, \quad (13)$$

where

$$\int_0^a \int_0^b u_{mn}u_{m'n'}^* \,\mathrm{d}x_0 \,\mathrm{d}y_0$$

$$= \int_0^a \int_0^b \left[\frac{\mathrm{j}\omega F \varphi_{mn}(x_0, y_0)}{[\omega_{mn}^2(1+\mathrm{j}\eta)-\omega^2]M_{mn}} \frac{-\mathrm{j}\omega F^* \varphi_{m'n'}(x_0, y_0)}{[\omega_{m'n'}^2(1-\mathrm{j}\eta)-\omega^2]M_{m'n'}}\right]\mathrm{d}x_0 \,\mathrm{d}y_0. \quad (14)$$

Because of the orthogonality of the eigenfunctions, it can be seen from Eq. (14) that Eq. (13) can be simplified to

$$\bar{W} = \sum_{m=1}^{\infty}\sum_{n=1}^{\infty}\left\{\frac{1}{ab}\int_0^a \int_0^b u_{mn}u_{mn}^* dx_0 dy_0 \int_0^{2\pi}\int_0^{\pi/2} \frac{A_{mn}(\mathbf{r})A_{mn}^*(\mathbf{r})}{2\rho c} r^2 \sin\theta \,\mathrm{d}\theta \,\mathrm{d}\phi\right\}, \quad (15)$$

where each term in the sum is the power radiated by a single mode. Hence the cross-modal terms have been eliminated. After some algebraic manipulations, Eq. (15) can also be written as

$$\bar{W} = \sum_{m=1}^{\infty}\sum_{n=1}^{\infty} \bar{W}_{mn}, \quad (16)$$

where $\bar{W}_{mn}$ is given by

$$\bar{W}_{mn} = \overline{|u_{mn}|^2} \int_0^{2\pi}\int_0^{\pi/2} \frac{A_{mn}(\mathbf{r})A_{mn}^*(\mathbf{r})}{2\rho c} r^2 \,\mathrm{d}\theta \,\mathrm{d}\phi \quad (17)$$

and $\overline{|u_{mn}|^2}$ represents the modulus squared of the modal velocity amplitude u_{mn}, averaged over all force positions. This is given by

$$\overline{|u_{mn}|^2} = \frac{1}{ab}\int_0^a \int_0^b u_{mn}u_{mn}^* \,\mathrm{d}x_0 \,\mathrm{d}y_0 = \frac{4\omega^2|F|^2}{M^2[(\omega_{mn}^2-\omega^2)^2+\eta^2\omega_{mn}^4]}. \quad (18)$$

The modal radiation efficiency σ_{mn} is hence given by

$$\sigma_{mn} = \frac{\bar{W}_{mn}}{\rho c a b \langle \overline{\overline{v_{mn}^2}} \rangle} = \frac{4 \int_0^{2\pi}\int_0^{\pi/2} A_{mn}(\mathbf{r})A_{mn}^*(\mathbf{r}) r^2 \,\mathrm{d}\theta \,\mathrm{d}\phi}{(\rho c)^2 ab}, \quad (19)$$

where $\overline{\langle \overline{v_{mn}^2} \rangle}$ represents the spatially averaged mean square velocity in mode (m, n) averaged over all possible force positions, which is given by

$$\overline{\langle \overline{v_{mn}^2} \rangle} = \frac{1}{S}\int_S \langle \overline{v_{mn}^2} \rangle \, \mathrm{d}x_0 \, \mathrm{d}y_0 = \frac{1}{2M^2}\frac{\omega^2|F|^2}{[(\omega_{mn}^2-\omega^2)^2+\eta^2\omega_{mn}^4]}. \tag{20}$$

After some algebraic manipulations to Eq. (19), the modal radiation efficiency σ_{mn} can be given by

$$\sigma_{mn} = \frac{64k^2ab}{\pi^6 m^2 n^2}\int_0^{\pi/2}\int_0^{\pi/2}\left\{\frac{\begin{matrix}\cos\\ \sin\end{matrix}(\alpha/2)\begin{matrix}\cos\\ \sin\end{matrix}(\beta/2)}{[(\alpha/(m\pi))^2-1][(\beta/(n\pi))^2-1]}\right\}^2 \sin\theta \, \mathrm{d}\theta \, \mathrm{d}\phi \tag{21}$$

which corresponds to the expression given by Wallace [3].

Having obtained the total radiated power in terms of a summation of modal radiated power, the average radiation efficiency considering all possible point force locations is readily given from Eq. (1) by

$$\sigma = \frac{\sum_{m=1}^{\infty}\sum_{m=1}^{\infty}\bar{W}_{mn}}{\rho cab\overline{\langle \overline{v^2} \rangle}} = \frac{\sum_{m=1}^{\infty}\sum_{n=1}^{\infty}\rho cab\sigma_{mn}\overline{\langle \overline{v_{mn}^2} \rangle}}{\rho cab\overline{\langle \overline{v^2} \rangle}} = \frac{\sum_{m=1}^{\infty}\sum_{n=1}^{\infty}\sigma_{mn}\overline{\langle \overline{v_{mn}^2} \rangle}}{\overline{\langle \overline{v^2} \rangle}}, \tag{22}$$

where $\overline{\langle \overline{v^2} \rangle}$ is the spatially averaged mean square velocity averaged over all possible force locations. This is given by [16]

$$\overline{\langle \overline{v^2} \rangle} = \frac{\omega^2|F|^2}{2M^2}\sum_{m=1}^{\infty}\sum_{n=1}^{\infty}\frac{1}{[(\omega_{mn}^2-\omega^2)^2+\eta^2\omega_{mn}^4]} = \sum_{m=1}^{\infty}\sum_{n=1}^{\infty}\overline{\langle \overline{v_{mn}^2} \rangle}. \tag{23}$$

Hence,

$$\sigma = \frac{\sum_{m=1}^{\infty}\sum_{n=1}^{\infty}\sigma_{mn}[(\omega_{mn}^2-\omega^2)^2+\eta^2\omega_{mn}^4]^{-1}}{\sum_{m=1}^{\infty}\sum_{n=1}^{\infty}[(\omega_{mn}^2-\omega^2)^2+\eta^2\omega_{mn}^4]^{-1}}. \tag{24}$$

It is noted that this average radiation efficiency depends only on the self-modal radiation due to the averaging over all possible force locations. Eq. (22) is stated by Cremer and Heckl [16], who analyzed the radiated power using a wavenumber transform but without explicitly averaging over excitation points. However, as shown here, it is only strictly valid when such averaging is included.

Using the modal summation approach, based on Eq. (22), various values of the damping of the plate can be taken into account.

3. Comparison with conventional modal average results

3.1. Example results

Based on Eq. (22), the average radiation efficiency of a rectangular plate of dimensions $0.5 \times 0.6 \times 0.003$ m is calculated as an example. The plate is chosen as aluminium with Young's

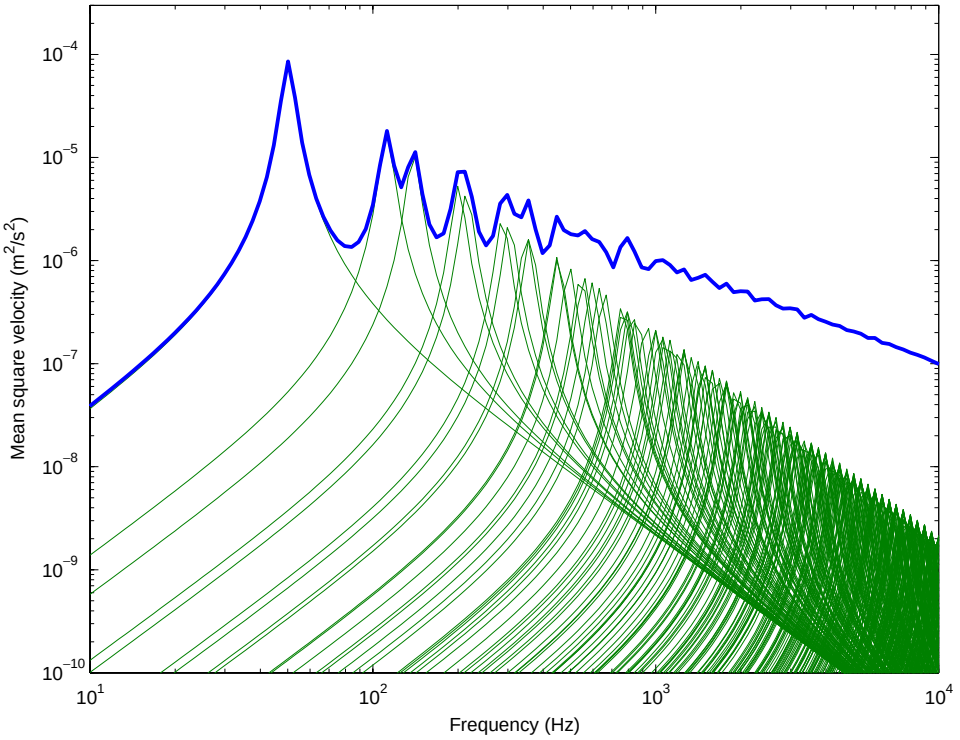

Fig. 2. Average mean square velocity of a rectangular plate showing contribution from modes ($0.6 \times 0.5 \times 0.003$ m aluminium plate with $\eta = 0.1$): —, modal mean square velocity; ▬, total mean square velocity.

modulus $7.1 \times 10^{10}\,\mathrm{N/m^2}$, density $2700\,\mathrm{kg/m^3}$ and a damping loss factor $\eta = 0.1$. This level of damping is used here for clarity although other values of damping are considered later. Calculations are implemented using 40 frequency points per decade that ensure 3 points within the half-power bandwidth of resonances.

Fig. 2 presents the spatially averaged mean square velocity from Eq. (23) and the spatially averaged mean square velocity for each mode from Eq. (20) for the rectangular plate with a unit force amplitude. The infinite numbers of modes in these two equations are truncated to a finite number. For this example rectangular plate, all modes with natural frequencies below 10 kHz are included in the calculation.

Fig. 3 presents the modal and average radiation efficiency of the above rectangular plate. It can be seen that below 70 Hz the radiation efficiency of the first mode determines the overall result. This is due to the dominance of this mode in the response, see Fig. 2, and its high value of σ_{mn}. Above this frequency the average result drops, only rising to 1 at the critical frequency (see below) of about 4 kHz.

3.2. Conventional modal average results

Based on the assumption of a diffuse field in the plate, Maidanik [2] has produced formulae for the modal-average radiation of a lightly damped plate. These can be

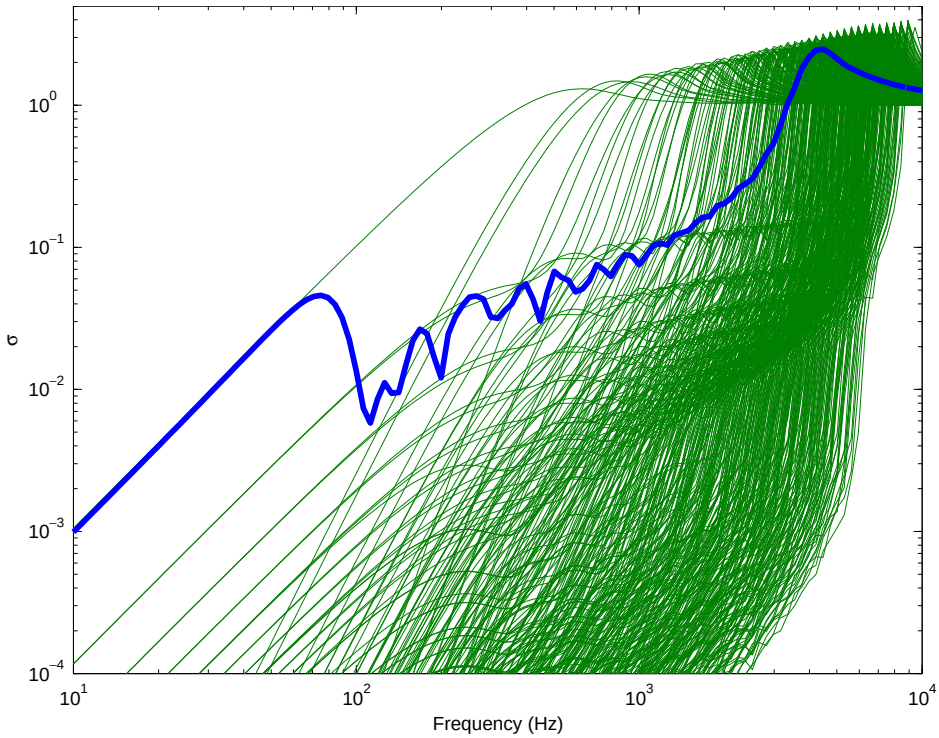

Fig. 3. Modal and average radiation efficiency of a rectangular plate ($0.6 \times 0.5 \times 0.003$ m aluminium plate with $\eta = 0.1$): —, modal radiation efficiency; ▬, average radiation efficiency.

written as [10]

$$\sigma = \begin{cases} \dfrac{4S}{c^2} f^2 & \text{for } f < f_{1,1}, \\ \dfrac{4\pi^2}{c^2 S} \dfrac{B}{m''} & \text{for } f_{1,1} < f < f_e,\ f_e = \dfrac{3c}{P}, \\ \dfrac{Pc}{4\pi^2 S f_c} \times \dfrac{(1-\alpha^2)\ln\left(\dfrac{1+\alpha}{1-\alpha}\right) + 2\alpha}{(1-\alpha^2)^{3/2}} & \text{for } f_e < f < f_c,\ \alpha = \sqrt{\dfrac{f}{f_c}}, \\ 0.45\sqrt{\dfrac{P f_c}{c}} & \text{for } f = f_c, \\ \left(1 - \dfrac{f_c}{f}\right)^{-1/2} & \text{for } f > f_c, \end{cases} \tag{25}$$

where c is speed of sound, f is frequency, P is the perimeter of the plate, S is the area of the plate, $f_{1,1}$ is the first resonance frequency of the plate, B is the bending stiffness, m'' is the mass per unit area of the plate and f_c is the critical frequency, $f_c = (m''/B)^{1/2} c^2/2\pi$. The first and second terms

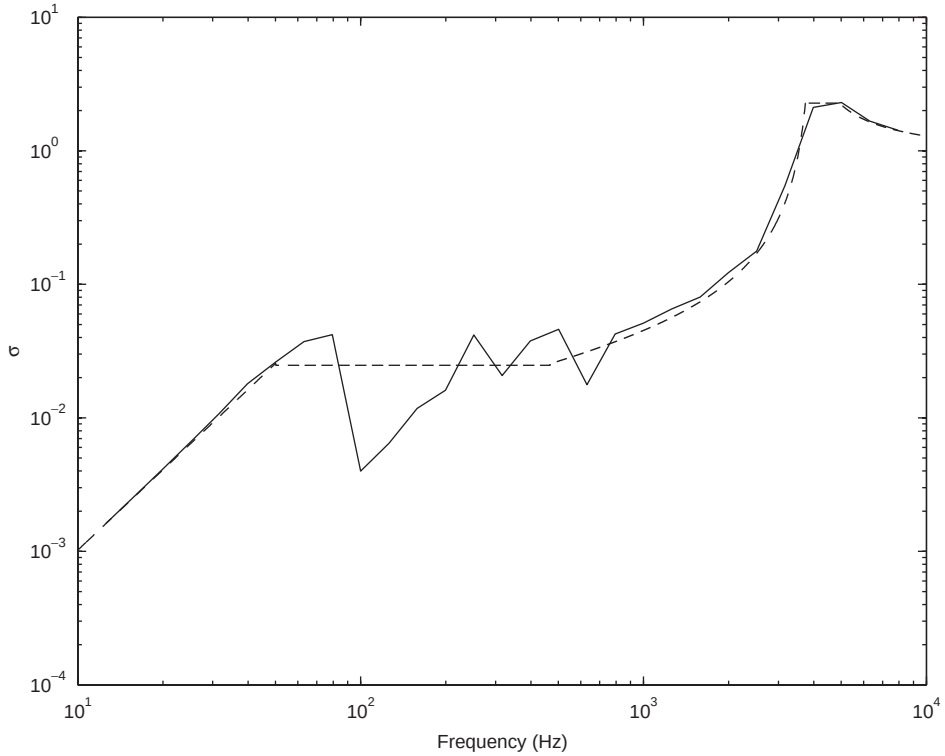

Fig. 4. Average radiation efficiency of a rectangular plate ($0.6 \times 0.5 \times 0.003$ m aluminium plate with $\eta = 0.0005$): —, average radiation efficiency from the modal summation approach; – –, Eq. (25).

have been added here from Ref. [10] to represent the monopole radiation from the motion below the first resonance frequency and radiation in the so-called corner mode region. NB, an additional term in the third expression is presented in Ref. [2] but is often omitted, see also Ref. [17].

Fig. 4 presents a comparison of the results from Eq. (25) and the modal summation approach. The same plate is used as above but now has a damping loss factor 0.0005. The calculation is carried out using 4000 points per decade. The curve shown in Fig. 4 has been converted into one-third octave bands for clarity. The comparison shows that Eq. (25) gives a good agreement with the numerical result at almost all frequencies. There is some fluctuation of the numerical result between the fundamental natural frequency (at 50 Hz) and about 500 Hz. It is well known that this frequency range is dominated by 'corner' modes (modes with $ka \ll 1$ and $kb \ll 1$). For these modes sound radiation is effectively limited to the corners of the plate and the radiation efficiency is approximately constant with frequency. As frequency increases, the radiation efficiency increases until the critical frequency. This increasing region corresponds to the occurrence of 'edge' modes ($ka < 1$, $kb > 1$ or $ka > 1$, $kb < 1$) where radiation is from two opposite edges [17].

3.3. Inclusion of nearfield effects

Cremer, Heckl and Ungar [16] and Fahy [17] have given analyses for the sound radiation from the vibration nearfield around the forcing point for a damped rectangular plate. From this, the

equivalent radiation efficiency from the nearfield of a point force can be expressed as

$$\sigma_n = \frac{4}{\pi}\frac{f}{f_c}\eta \quad \text{for } f < f_c. \tag{26}$$

The power radiated is obtained using this value of σ with the mean square velocity of the whole plate. The overall radiation efficiency of a damped point-excited plate can thus be given by

$$\sigma = \sigma_0 + \sigma_n \quad \text{for } f < f_c, \tag{27}$$

where σ_0 is the radiation efficiency for very lightly damped plates, which is given by Eq. (25).

The result from Eq. (27) agrees well with that from the modal summation approach. Fig. 5 presents the results for three values of the damping loss factor. It can be seen that the radiation efficiency is independent of the damping loss factor for frequencies below the fundamental natural frequency and above the critical frequency, but depends on the loss factor in the corner and edge mode region. This increase in radiation efficiency is proportional to the damping loss factor this can also be understood qualitatively in terms of the modal summation approach. Due to the increase in the damping, the amplitude of the modal response at resonance to a point force decreases. So does the spatially averaged mean square velocity. Hence relatively more modes will contribute significantly to the response in this frequency range so that average radiation efficiency increases.

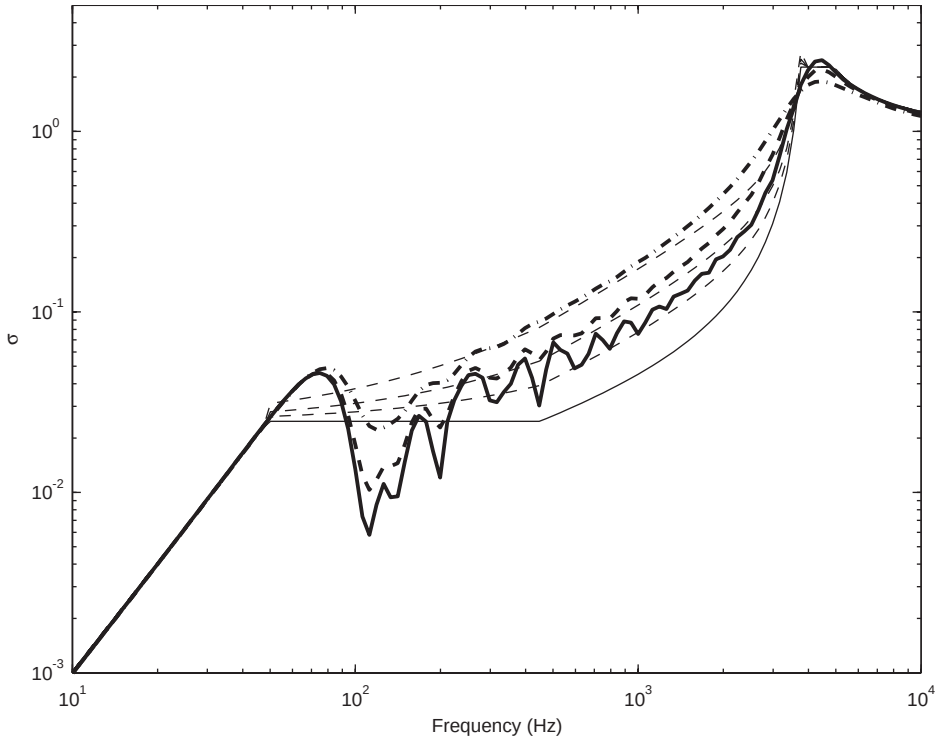

Fig. 5. The average radiation efficiency from the modal summation and Eq. (27). ——, $\eta = 0.1$; – –, $\eta = 0.2$; ·——·, $\eta = 0.4$; —, formula by Maidanik; – –, Eq. (27).

It is also noted from Cremer et al. [16] that, when the radiated power is studied, the power radiated by the nearfield does not depend on the damping loss factor whereas the modal response does. The increase in radiation efficiency with increase in damping is, in effect, due to the reduction in the modal response and thus the greater importance of the nearfield.

3.4. Radiation efficiency at the critical frequency

The radiation efficiency at the critical frequency, given in Eq. (25), can also be represented in terms of the non-dimensional parameter $k_c a$ as

$$\sigma = 0.45(k_c a)^{1/2}\left(\frac{\gamma+1}{\gamma\pi}\right)^{1/2}, \tag{28}$$

where k_c is the wavenumber at the critical frequency, a is the length of the shorter edges of the plate (i.e., $a \leqslant b$), γ denotes the ratio of the lengths of shorter edges to longer edges $\gamma = a/b$.

Leppington [7] found that Eq. (28) overestimates the radiation efficiency for plates with large aspect ratios and presented a modified formula as

$$\sigma = (k_c a)^{1/2} H(\gamma), \tag{29}$$

where k_c, a and γ have the same meaning as in Eq. (28) and the function $H(\gamma)$ is given by

$$H(x) = \frac{4}{15\pi^{3/2}} x^{1/2} \int_0^1 (5-t)\left\{(t^2+x^2)^{-3/4} + (1+x^2t^2)^{-3/4}\right\} \mathrm{d}t. \tag{30}$$

For $0.2 < x < 1$, a good approximation of $H(x)$ is given by $H(x) = 0.5 - 0.15x$.

It can be noted that, for a given aspect ratio, both Eqs. (28) and (29) will give a value of radiation efficiency for the critical frequency smaller than unity for $k_c a$ smaller than a certain value. For instance, Eq. (28) gives results less than unity for $k_c a \leqslant 7.6$ for $\gamma = 1$ and $k_c a \leqslant 2.6$ for $\gamma = 0.2$ while Eq. (29) for $k_c a \leqslant 7.6$ for $\gamma = 1$, $k_c a \leqslant 4.2$ for $\gamma = 0.2$. Thick, stiff (or small) plates can have a critical frequency near to, or lower than, their first natural frequency, corresponding to a small value of $k_c a$. In this case, Eqs. (28) and (29) are not appropriate to estimate the radiation efficiency. At their 'critical frequency' these plates vibrate as piston which is small compared with the acoustic wavelength and therefore radiate inefficiently. The concept of critical frequency is not meaningful in this context.

Using the modal summation approach of Section 2, the radiation efficiencies at the critical frequency have been reinvestigated. Fig. 6 presents a comparison of the results from modal summation and according to Eqs. (28) and (29) for square plates ($\gamma = 1$). For square plates, Eqs. (28) and (29) give similar results to each other. Results are given for two values of damping loss factor for the plate. The results presented from the modal summation are the maximum radiation efficiency, which occurs around, or just above, the critical frequency. Both narrow band (300 frequency points per decade) and one-third octave band results from the modal summation are plotted. The latter are included since predictions are often made in one-third octave bands, in which case the precise details of a narrow peak are less important than the frequency average behaviour. The one-third octave band here is centred about the frequency at which the maximum radiation efficiency occurs.

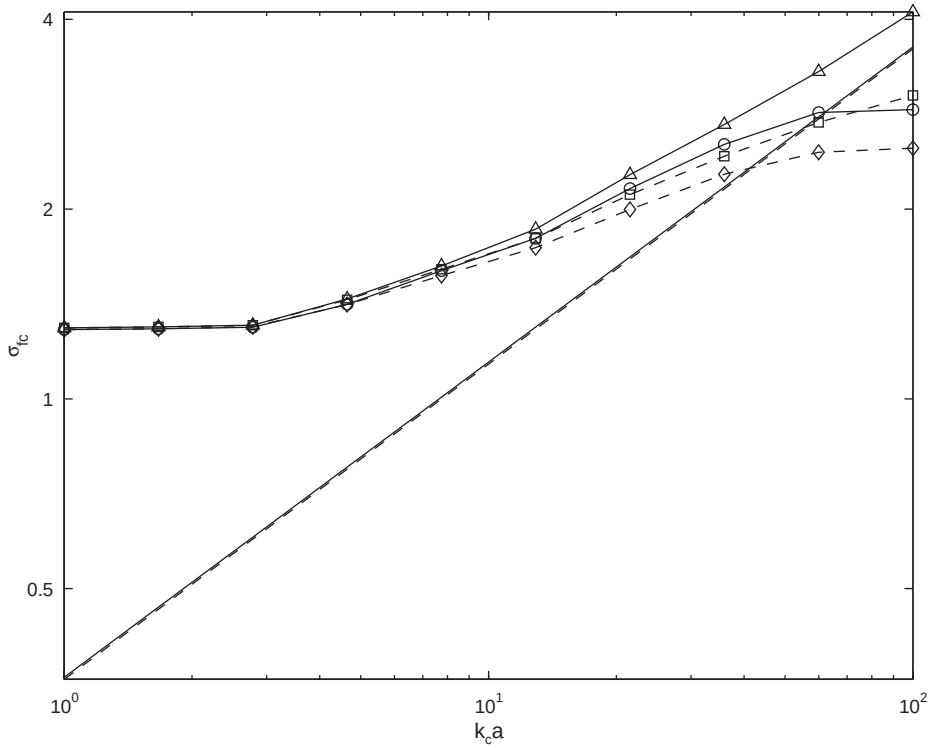

Fig. 6. Maximum radiation efficiencies from modal summation. $\gamma = 1$, damping loss factor 0.01; –○–, one-third octave; –Δ–, narrow band; —, Eq. (29), – – , Eq. (28); –◇–, one-third octave $\eta = 0.1$; –□–, narrow band $\eta = 0.1$.

For large values of $k_c a$, the maximum value from the narrow band results is larger than that from one-third octave bands. The narrow band results for $\eta = 0.01$ appear to tend towards the approximate results for very large values of $k_c a$, but the result from one-third octave bands is lower than this at large $k_c a$. Damping does have certain effects on the results from the modal summation approach. Fig. 6 includes corresponding results for a damping loss factor of 0.1. The radiation efficiency at the critical frequency will decrease as the damping loss factor increases for large values of $k_c a$. As damping increases, the response differs increasingly from a free wave of wavelength equal to the acoustic wavelength, and the coincidence effect will reduce. For $k_c a$ smaller than 10, the radiation efficiency at the critical frequency is largely independent of damping loss factor, as here the boundaries disturb the coincidence phenomenon to a greater extent.

For $k_c a$ smaller than 3, the maximum radiation efficiency tends to a constant value of 1.3 that is actually determined by the maximum modal radiation efficiency of the fundamental mode (see Fig. 3) rather than the result at the critical frequency. Fig. 7 presents examples of the average radiation efficiencies of square plates with different thickness and $\eta = 0.01$ calculated using the modal summation approach. In each case the critical frequency is also marked. For the thickest plate shown, the maximum radiation efficiency is not associated with the critical frequency. As the thickness reduces the maximum value occurs at frequencies that are progressively closer to the corresponding critical frequency.

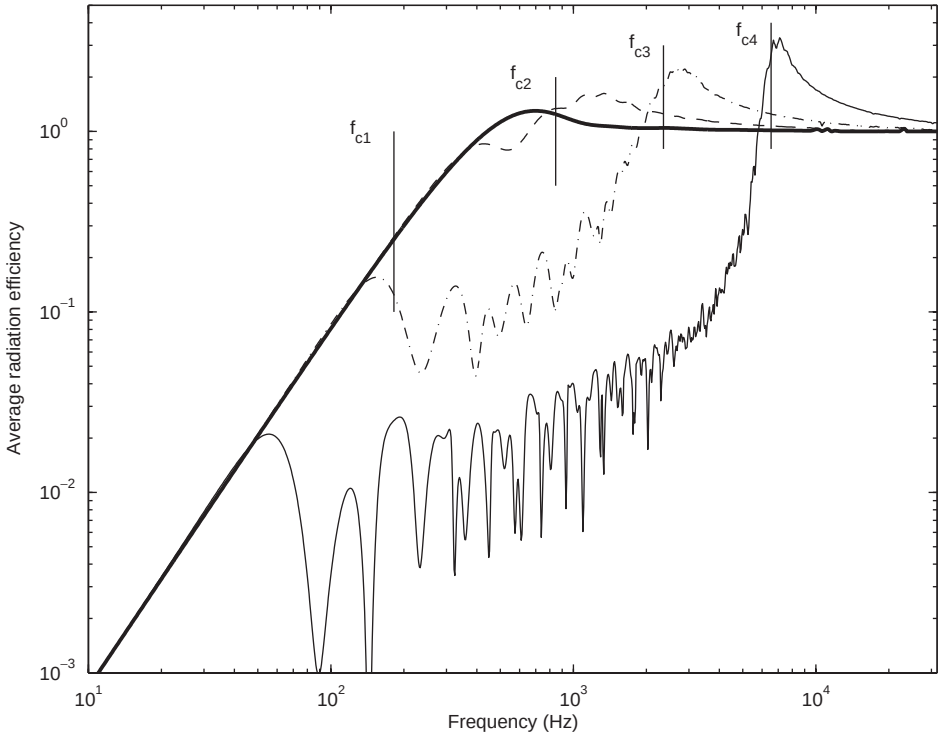

Fig. 7. Average radiation efficiency of plate 0.5×0.5 m with several different thickness, $\eta = 0.01$ (—, h= 1.8 mm, $k_c a = 60.0$; · — ·, h= 5.1 mm, $k_c a = 21.5$; – –, h = 14 mm, $k_c a = 7.74$; ▬, h= 66 mm, $k_c a = 1.67$).

Corresponding investigations have been carried out for a plate with $\gamma = 0.2$. Fig. 8 presents the comparison of the results from modal summation and Eqs. (28) and (29). Damping loss factors of 0.01 and 0.1 again are used in these calculations. For large $k_c a$, Eq. (29) slightly overestimates the radiation efficiency at the critical frequency compared with the result from the modal summation. The result from Eq. (28) is higher still. For $k_c a$ smaller than 2, the maximum radiation efficiency tends to a constant value (1.2) as before. Results were not produced for larger values of $k_c a$ due to the very long computation times required, but it can be anticipated that they will drop below the lines corresponding to the approximate formula.

In order to find a general relation between the maximum average radiation efficiency and the value of $k_c a$, the analysis has been extended to include plates with different values of γ. Fig. 9 shows the results for seven different aspect ratios obtained from the modal summation. All the results are given in one-third octave bands. For $k_c a < 3$, the radiation efficiency tends to a constant value between 1.2 and 1.3 for different aspect ratios, determined by the modal radiation efficiency of the fundamental mode. For $k_c a > 3$, the radiation efficiency increases approximately in proportion to $(k_c a)^{1/4}$, rather than $(k_c a)^{1/2}$ as given in Eqs. (28) and (29). Moreover the result appears to be only weakly dependent on the aspect ratio as Fig. 10 shows. These results can be summarized by an approximate

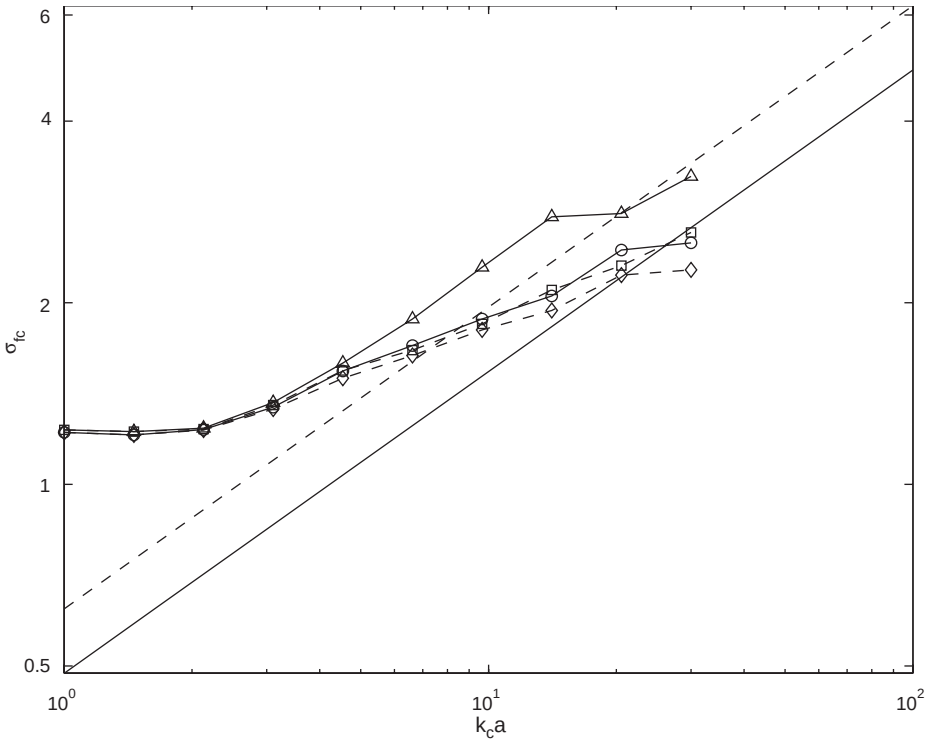

Fig. 8. Maximum radiation efficiencies from modal summation ($\gamma = 0.2$) –○–, one-third octave $\eta = 0.01$, –Δ–, narrow band; $\eta = 0.01$, ——, Eq. (29); – –, Eq. (28); –◇–, one-third octave band $\eta = 0.1$; –□–, narrow band $\eta = 0.1$.

expression as

$$\sigma_c \approx \begin{cases} 1.2 - 1.3 & \text{for } k_c a \leqslant 3, \\ (k_c a)^{1/4} & \text{for } k_c a > 3. \end{cases} \tag{31}$$

4. Radiation efficiency of strips

4.1. Results from the modal summation approach

Next the modal summation approach technique, described in Section 2, is used to study the radiation from a strip, that is a plate with a large aspect ratio, or small value of γ.

Fig. 11 presents the average mean square velocity for a unit force amplitude of a plate with dimensions $0.16 \times 3.0 \times 0.003$ m as a sum of the individual modal contributions in a manner similar to Fig. 2. A damping loss factor $\eta = 0.1$ is used. This plate has an aspect ratio $\gamma = 0.053$. The natural frequencies of the strip can be seen as the peaks of the modal amplitudes in Fig. 11. At about 290 Hz, the first mode corresponding to a half-wavelength of bending along the strip occurs (the fundamental mode, in which $m = 1$, $n = 1$). Above this frequency, modes of higher order (index n) bending waves along the strip occur close together in frequency. Just above

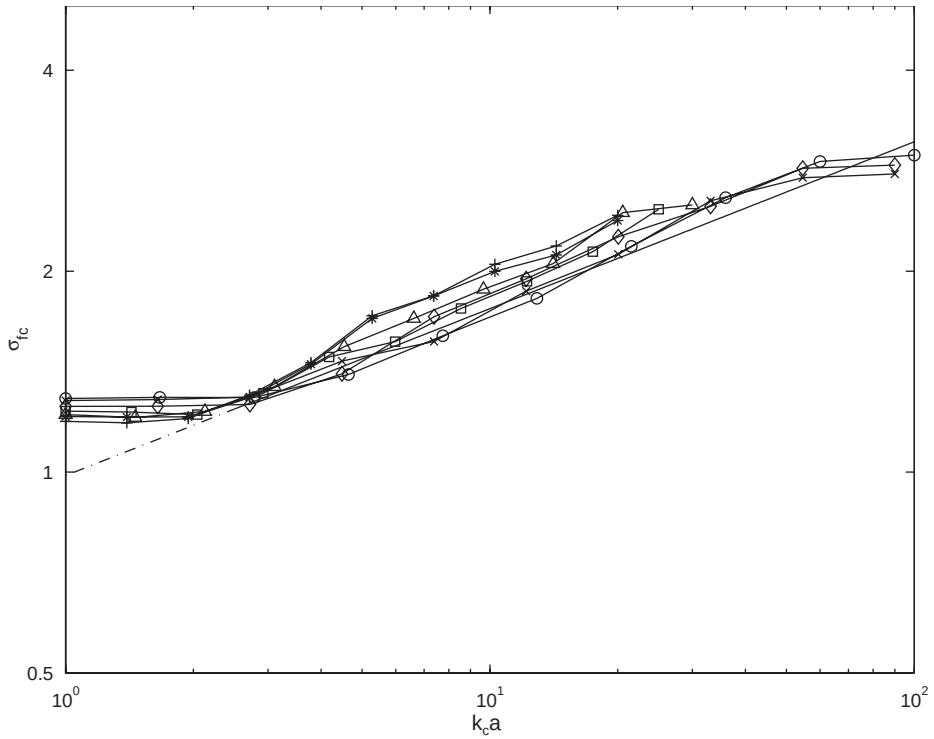

Fig. 9. Radiation efficiencies at the critical frequencies from modal summation for different aspect ratios in one-third octave band for $\eta = 0.01$ (thick line, Eq. (31); $-\bigcirc-$, $\gamma = 1$; $-\times-$, $\gamma = 0.8$; $-\diamond-$, $\gamma = 0.6$; $-\square-$, $\gamma = 0.4$; $-\Delta-$, $\gamma = 0.2$; $-*-$, $\gamma = 0.1$; $-+-$, $\gamma = 0.16/3$).

1.1 kHz, the first mode corresponding to a whole wavelength of bending across the strip occurs ($m = 2$). Above this 'cut-on' frequency of order $m = 2$, modes with $n = 1, 2, 3, \ldots$ occur closely spaced. At about 2.6 kHz, modes of order $m = 3$ can be seen to cut-on.

Fig. 12 presents both the modal radiation efficiency and average radiation efficiency calculated using the modal summation approach. The curve of average radiation efficiency of the strip has two broad peaks, which occur close to the fundamental mode (1, 1) and close to the second mode along the short edge (2, 1). If Eq. (25) is used to evaluate the average radiation efficiency for the strip, a significant underprediction is made above the first mode. This is shown in Fig. 13. Even including the result of damping using Eq. (27) does not account for the behaviour correctly. Moreover, below the fundamental mode, the radiation efficiency is considerably lower than given by Eq. (25). Only at frequencies well above the critical frequency is the formula able to predict the radiation efficiency well for the strip. Clearly, further investigation is required into the radiation behaviour of such a very narrow rectangular plate.

4.2. *Below the fundamental frequency*

The modes with odd indices (both m and n) are the most effective radiators for a rectangular plate when ka, $kb \ll 1$ [2,3]. For frequencies well below the fundamental natural frequency, the

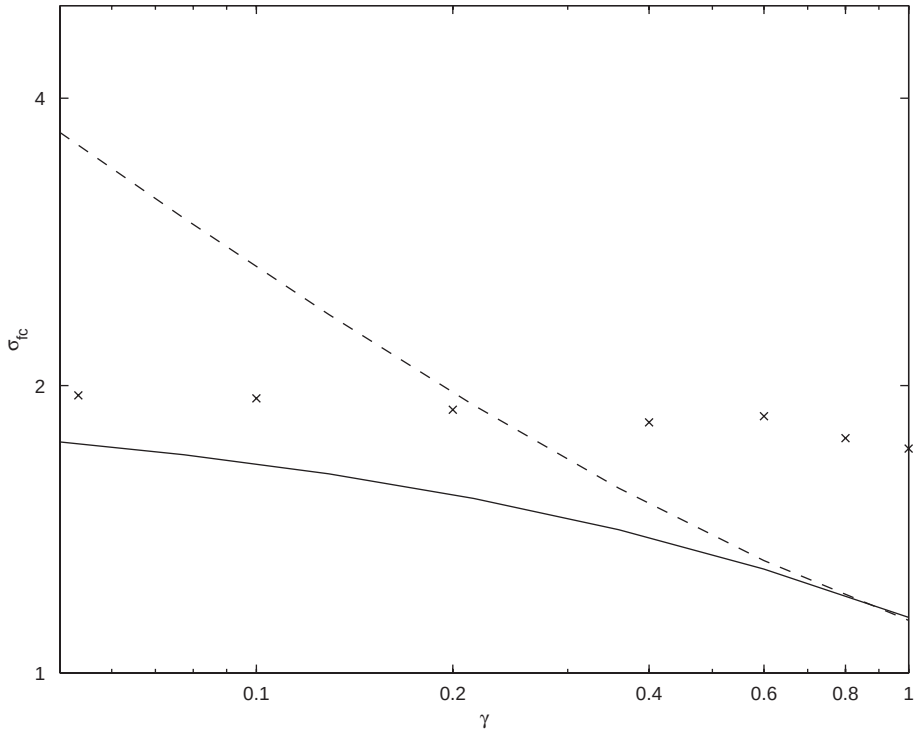

Fig. 10. Maximum radiation efficiencies from modal summation for $k_c a = 10$. ×, modal summation; —, Eq. (29); – –, Eq. (28).

average radiation efficiency of a plate with moderate aspect ratio is dominated by the fundamental mode (see Fig. 3). This is not only because the radiation of the fundamental mode is most effective but also because its velocity amplitude is dominant (see Eq. (20) and Fig. 2). The summation in both the denominator and numerator of Eq. (22) is dominated by the term corresponding to the fundamental mode. Therefore the average radiation efficiency of this plate below the fundamental natural frequency can be given by

$$\sigma \approx \frac{\sigma_{1,1}\overline{\langle \overline{v_{1,1}^2} \rangle}}{\overline{\langle \overline{v_{1,1}^2} \rangle}} = \sigma_{1,1}. \tag{32}$$

The physical explanation of Eq. (32) is that the whole surface of the plate vibrates in phase in the form of the first mode and the plate motion radiates sound as a monopole.

However, the case of a strip differs from this because of its large aspect ratio. As a result of the large aspect ratio, many modes are distributed closely just above the fundamental frequency (see Fig. 11). From Eq. (20), it can be seen that the mean square velocity of these modes will have very similar amplitude since ω_{mn} is similar in each case. As a result, the approximation of Eq. (32) will no longer be valid. Suppose p modes have significant values that contribute to the average radiation efficiency below the fundamental frequency.

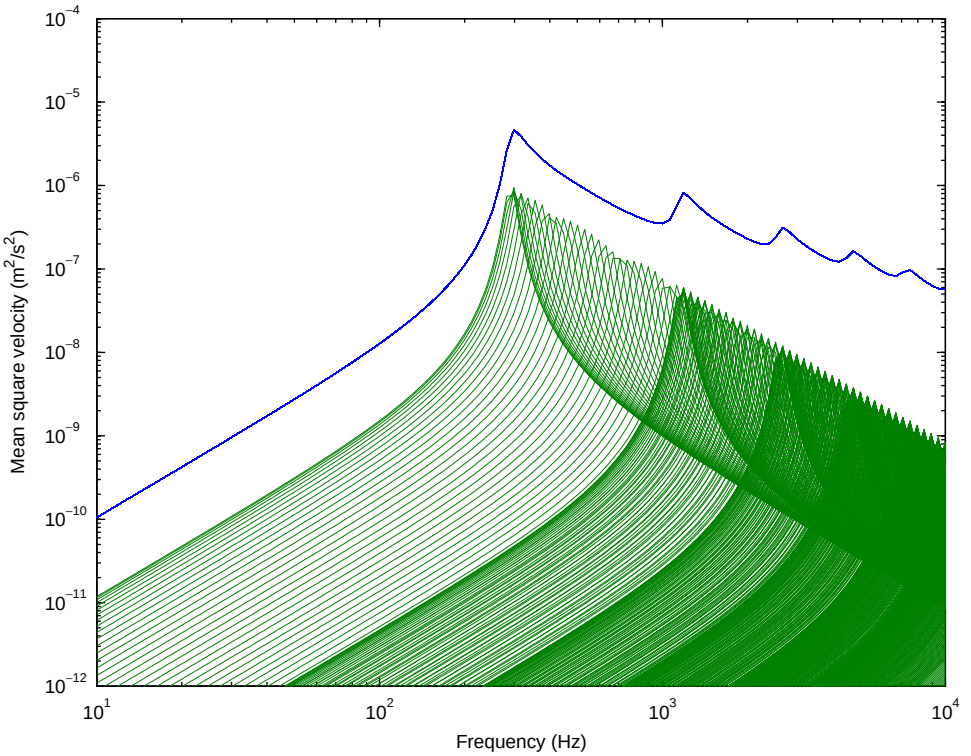

Fig. 11. Average mean square velocity of the strip showing contributions from modes. $0.16 \times 3 \times 0.003$ m aluminium strip with $\eta = 0.1$, —, Modal mean square velocity; ▬, total mean square velocity.

Then Eq. (22) should be rewritten as

$$\sigma \approx \frac{\sum_{n=1}^{p} \sigma_{1,n} \overline{\langle \overline{v_{1,n}^2} \rangle}}{\sum_{n=1}^{p} \overline{\langle \overline{v_{1,n}^2} \rangle}}. \tag{33}$$

Since the fundamental mode is the most effective in sound radiation, the numerator of Eq. (33) is still dominated by the term corresponding to the fundamental mode. Thus Eq. (33) can be simplified as

$$\sigma \approx \frac{\sigma_{1,1} \overline{\langle \overline{v_{1,1}^2} \rangle}}{\sum_{n=1}^{p} \overline{\langle \overline{v_{1,n}^2} \rangle}}. \tag{34}$$

It is now necessary to determine which modes of the strip will contribute to the average radiation efficiency. The mean square velocity of the mode (m, n) can be approximated by

$$\overline{\langle \overline{v_{m,n}^2} \rangle}(\omega) \approx \frac{\omega^2 |F|^2}{2M^2 \omega_{m,n}^4 (1 + \eta^2)} \quad \text{for } \omega \ll \omega_{mn}. \tag{35}$$

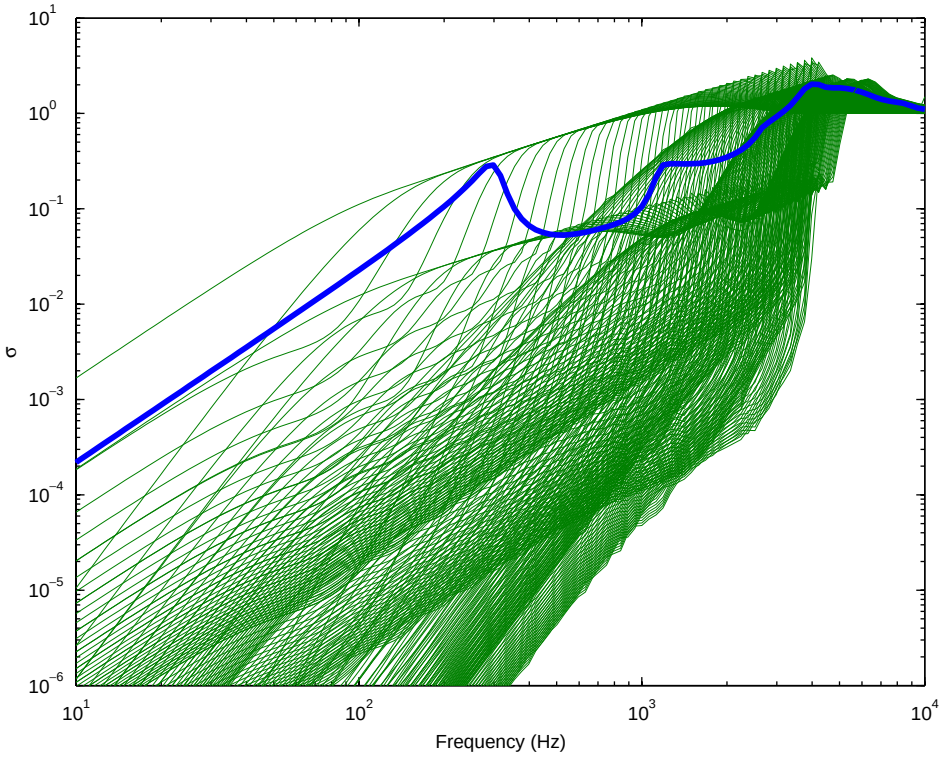

Fig. 12. Modal and average radiation efficiency of the $0.16 \times 3 \times 0.003$ m aluminium strip with $\eta = 0.1$. —, Modal radiation efficiency; ▬, average radiation efficiency.

The ratio of the mean square velocity of mode $(1,n)$ to that of the fundamental mode is given by

$$\frac{\overline{\langle \overline{v_{1,n}^2} \rangle}}{\overline{\langle \overline{v_{1,1}^2} \rangle}} = \left(\frac{\omega_{1,1}}{\omega_{1,n}}\right)^4, \tag{36}$$

where

$$\omega_{1,1} = \sqrt{\frac{B}{m''}}\left[\left(\frac{\pi}{a}\right)^2 + \left(\frac{\pi}{b}\right)^2\right], \quad \omega_{1,n} = \sqrt{\frac{B}{m''}}\left[\left(\frac{\pi}{a}\right)^2 + \left(\frac{n\pi}{b}\right)^2\right].$$

Writing $\Delta k_x = \pi/a$ and $\Delta k_y = \pi/b$, Eq. (36) can be rewritten as

$$\frac{\overline{\langle \overline{v_{1,n}^2} \rangle}}{\overline{\langle \overline{v_{1,1}^2} \rangle}} = \left(\frac{\Delta k_x^2 + \Delta k_y^2}{\Delta k_x^2 + n^2 \Delta k_y^2}\right)^4. \tag{37}$$

For the case of a strip with $a \ll b$, $\Delta k_y \ll \Delta k_x$ and writing $\gamma = a/b$, gives

$$\frac{\overline{\langle \overline{v_{1,n}^2} \rangle}}{\overline{\langle \overline{v_{1,1}^2} \rangle}} \approx \left(\frac{\Delta k_x^2}{\Delta k_x^2 (1 + \gamma^2 n^2)}\right)^4 \approx (1 + \gamma^2 n^2)^{-4}. \tag{38}$$

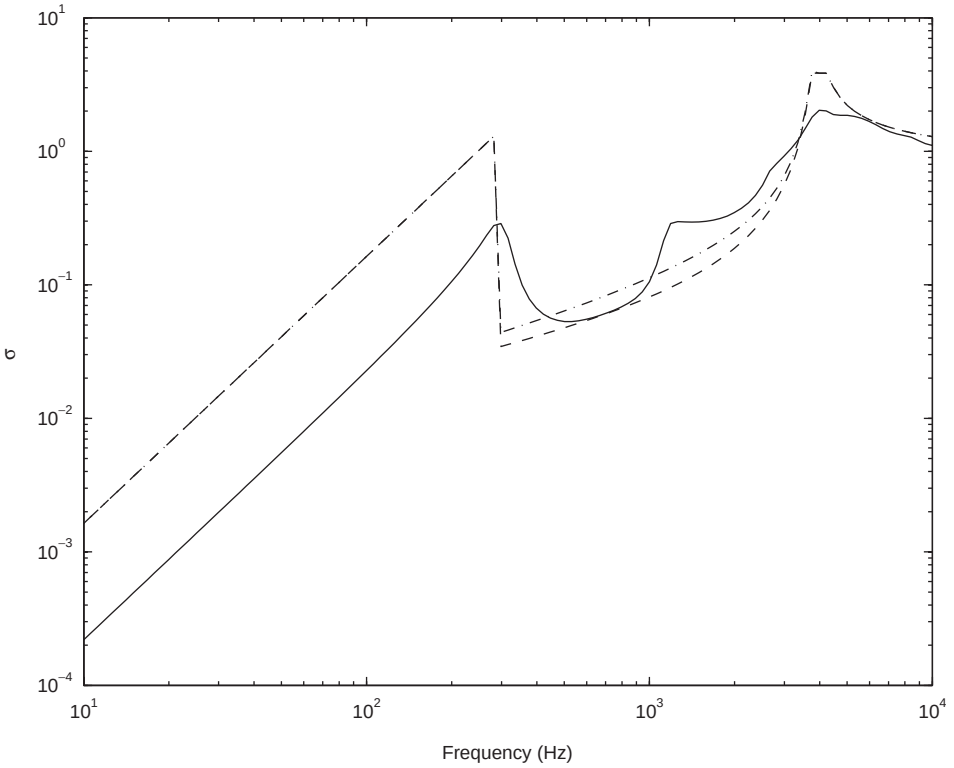

Fig. 13. Average radiation efficiency of the aluminium strip of $0.16 \times 3 \times 0.003$ m with $\eta = 0.1$. —, Modal summation approach; – –, Eq. (25); ·—·, Eq. (27).

The average radiation efficiency of the strip below the fundamental natural frequency can be rewritten as

$$\sigma = \frac{\sigma_{1,1}\overline{\langle \overline{v_{1,1}^2} \rangle}}{\sum_{n=1}^{p} \overline{\langle \overline{v_{1,1}^2} \rangle}(1+\gamma^2 n^2)^{-4}} = \frac{\sigma_{1,1}}{\sum_{n=1}^{p} (1+\gamma^2 n^2)^{-4}}. \tag{39}$$

It has been found by numerical evaluation that $\sum_{n=1}^{p}(1+\gamma^2 n^2)^{-4}$ can be approximated as

$$\sum_{n=1}^{p} (1+\gamma^2 n^2)^{-4} \approx 0.485\left(\frac{1}{\gamma} - 1\right) \quad \text{for } p \text{ large and } \gamma \leqslant 0.5. \tag{40}$$

Then the substitution of Eq. (40) into Eq. (39) gives

$$\sigma \approx \frac{\sigma_{1,1}}{0.485(1/\gamma - 1)}. \tag{41}$$

It can be noted that the average radiation efficiency of the strip depends on the aspect ratio and the radiation efficiency of the fundamental mode. Compared with the rectangular plate of the same area, the strip radiates less sound. In order to understand the characteristics of the strip

radiation physically, it is instructive to simplify Eq. (41) further as

$$\sigma \approx \frac{\gamma}{0.485}\sigma_{1,1} \quad \text{for } \gamma \leqslant 0.1. \tag{42}$$

According to Wallace [3], the radiation efficiency of the fundamental mode for frequencies well below the fundamental natural frequency can be approximately given by

$$\sigma_{1,1} = \frac{32(ka)(kb)}{\pi^5} = \frac{128}{\pi^3 c^2} abf^2. \tag{43}$$

This is proportional to the area of the plate. For the case of the strip, Eq. (42) gives

$$\sigma \approx \frac{1}{0.485}\frac{a}{b}\frac{128}{\pi^3 c^2} abf^2 \approx \frac{264}{\pi^3 c^2} a^2 f^2 \approx \frac{8.5}{c^2} a^2 f^2. \tag{44}$$

The average radiation efficiency of the strip at frequencies well below the first natural frequency is thus found to be approximately proportional to the square of the short-edge length of the strip and is independent of the long-edge length.

In order to verify this conclusion, strips with different aspect ratios have been investigated using the numerical evaluation of Eq. (22) and the modal radiation efficiency from the numerical integration of Eq. (21). Example calculations have been carried out for strips with a short edge

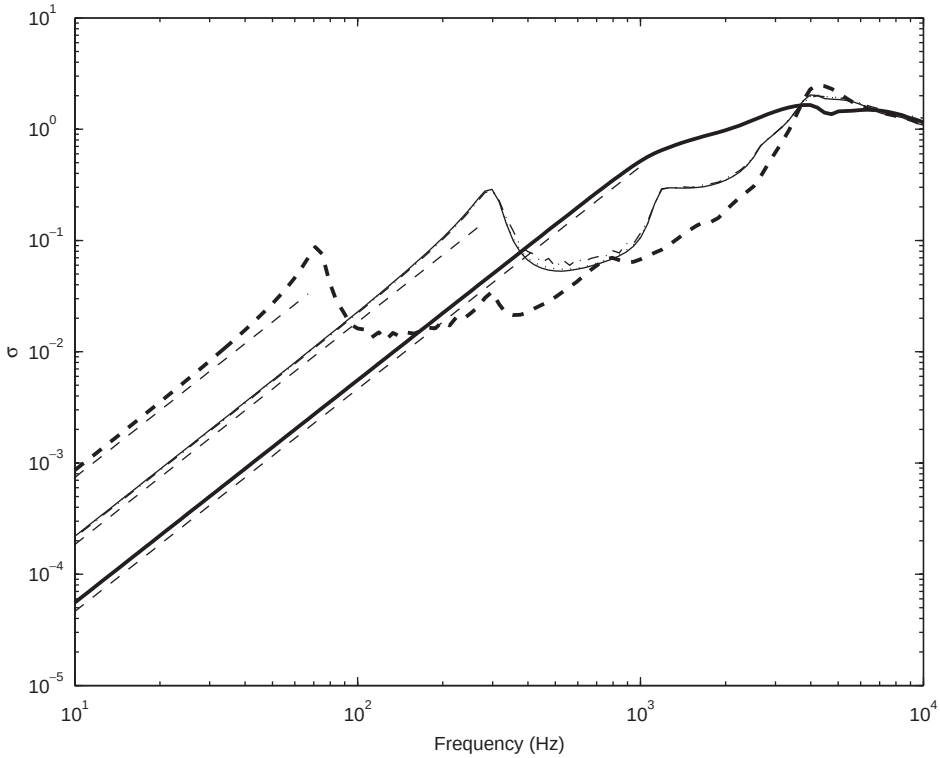

Fig. 14. Average radiation efficiency of aluminium strips $h = 0.003$ m, $\eta = 0.1$. —, 0.16×3 m; ·—·, 0.16×1.5 m, ···, 0.16×2.5 m; ▬, 0.08×3 m; ▬ ▬, 0.32×3 m; – –, from Eq. (44).

length of 0.16 m and long edge lengths of 1.5, 2.5 and 3 m and two additional strips with long edge length 3 m having short edge lengths of 0.08 and 0.32 m. The results are presented in Fig. 14. It is seen that the three strips with the same width, 0.16 m, have very similar average radiation efficiencies and are indistinguishable at low frequency. The results also verify that the average radiation efficiency below the fundamental natural frequency is proportional to the square of the short-edge length of the strip. Eq. (44) underestimates the average radiation efficiency slightly at low frequency if compared with the results from numerical calculations. This is because of the simplification from Eq. (33) to Eq. (34) by ignoring the contributions of other modes in the numerator. Actually, mode (1, 3) still has a significant contribution to the frequencies below the fundamental frequency.

4.3. Effects of damping

The average radiation efficiencies of the strip have been calculated for various damping values using the modal summation approach. These results are presented as one-third octave band spectra in Fig. 15. (The narrow band results vary too rapidly with frequency for clear observation to be made.) The average radiation efficiency is largely independent of the damping for frequencies below the fundamental natural frequency and above the critical frequency. However,

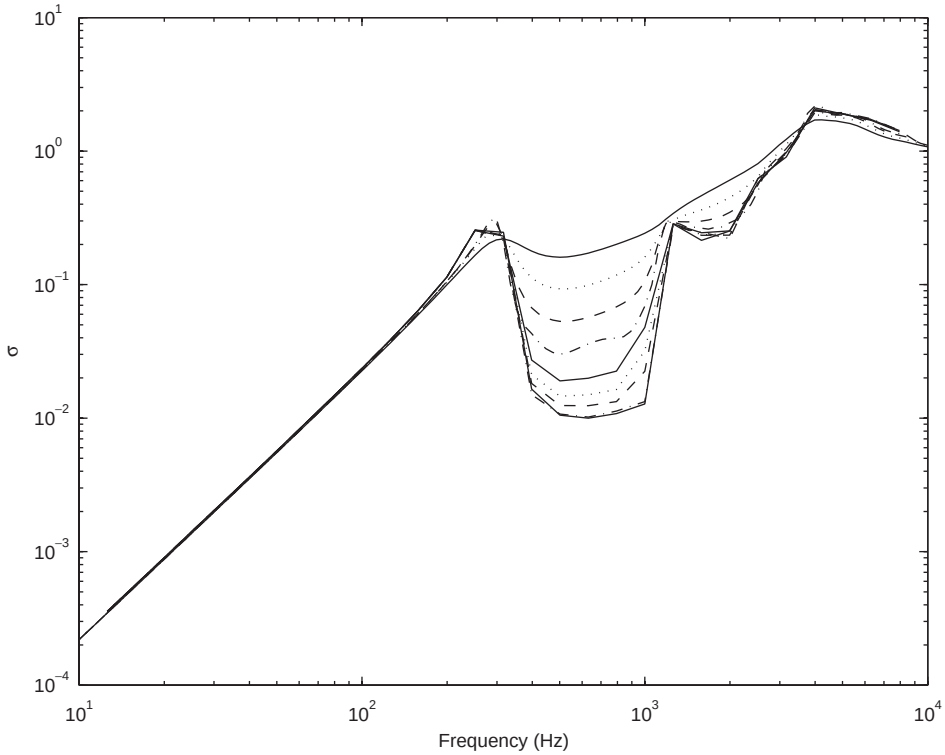

Fig. 15. Average radiation efficiency of an aluminium strip ($0.16 \times 3 \times 0.003$ m) with different damping values, 0.4, 0.2, 0.1, 0.05, 0.02, 0.01, 0.005, 0.001, 0.0005, respectively.

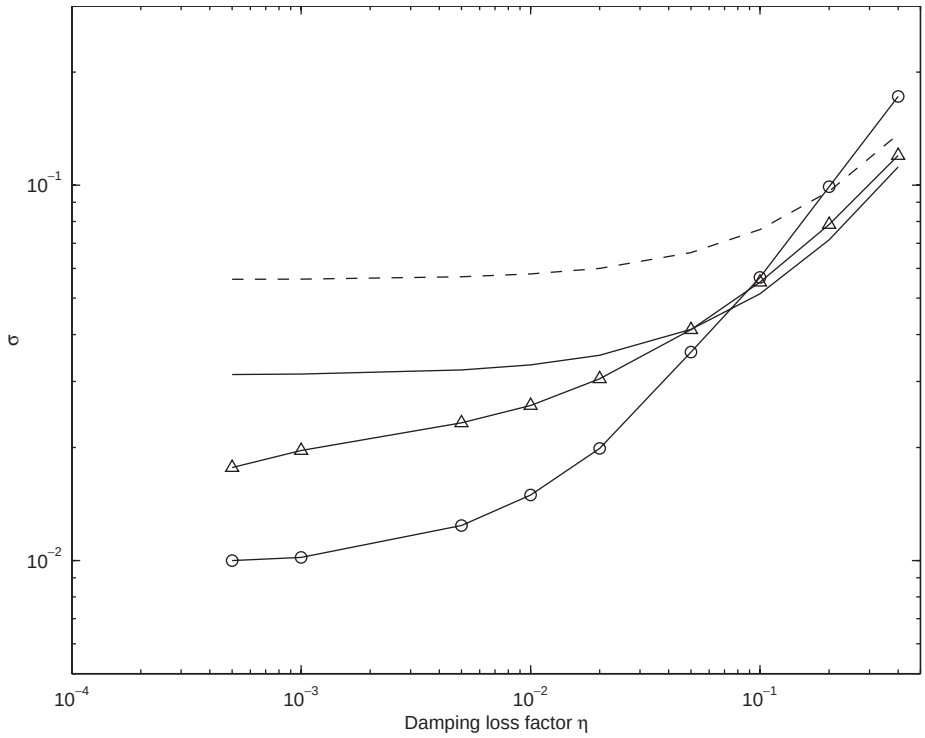

Fig. 16. Radiation efficiency in 630 Hz one-third octave band as a function of loss factor. –○–, Strip $0.16 \times 3 \times 0.003$ m by modal summation; –Δ–, rectangular plate $0.6 \times 0.5 \times 0.003$ m by modal summation; —, Eq. (27) for rectangular plate $0.6 \times 0.5 \times 0.003$ m; – –, Eq. (27) for strip.

the average radiation efficiency between the fundamental natural frequency and the critical frequency increases with an increase of damping. A quite large change occurs for the frequencies between the first two cut-on frequencies, where the radiation efficiency appears to be proportional to the damping loss factor. Fig. 16 shows the variation of the average radiation efficiency with loss factor for the example $0.16 \times 3.0 \times 0.003$ m strip in the 630 Hz band. Corresponding results for the rectangular plate considered previously with 0.6×0.5 m are shown for comparison. It can be seen that the radiation efficiency of the strip is much more strongly dependent on damping than that of the plate considered previously.

Fig. 17 shows the effect of damping on the approximated radiation efficiency using Eq. (27). The average radiation efficiency of the strip is shown for damping loss factors of 0.1, 0.2 and 0.4. These results are compared with the corresponding results from the modal summation. Not surprisingly, poor agreement is obtained. The cause of this disagreement can be attributed qualitatively to an overprediction in the modal radiation and an underprediction of the nearfield radiation.

The sparse distribution of the modes in k-space means that the assumption of a high modal density is not applicable and so Maidanik's formulae for calculating the average radiation efficiency for low damping may no longer be appropriate. This can be demonstrated in a comparison of the acoustic and structural wavenumbers, shown in Fig. 18. At the fundamental

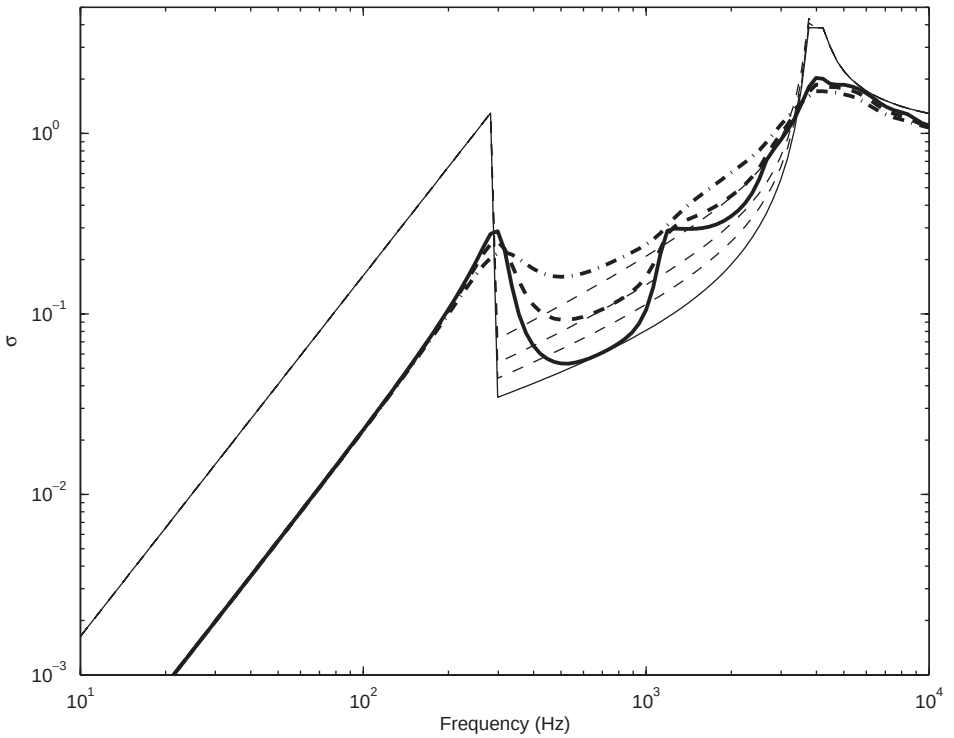

Fig. 17. Comparison of the average radiation efficiency for the strip between the modal summation and Eq. (27). ——, $\eta = 0.1$; – –, $\eta = 0.2$; ·—·, $\eta = 0.4$; —, Eq. (25); – –, Eq. (27).

natural frequency, the wavenumber in the plate is k_{b1} while that in air is k_{a1}, which is much smaller. The first few structural modes with $m = 1$ are 'edge' modes ($k_y < k_{a1}$), so the radiation at and just above the cut-on frequency is quite large. For a frequency between the first and second cut-on frequencies, k_{b2} is the wavenumber in the plate and k_{a2} is that in air. The radiation is now dominated by 'corner' modes ($k_y > k_{a2}$) and thus it is fairly low. For frequencies close to the second cut-on frequency, corresponding to k_{a3} for the acoustical wavenumber and k_{b3} for the structural one, the radiation is again controlled mainly by 'edge' modes. This causes another broad peak around this frequency. For frequencies above the second cut-on frequency, the distribution of modes becomes more even so that the average radiation efficiency formulae gradually become more appropriate with increasing frequency.

For the frequencies between the fundamental natural frequency and the second cut-on frequency, provided k_x, $k_y > k_a$, although the region has been called the 'corner mode region', the radiation from the strip can be considered to be equivalent to the radiation of two monopoles, each of size $a \times \lambda_y/4$ where λ_y is the wavelength along the length of the strip. Thus the 'corner' is spread over the whole width of the strip. The power radiated by the strip in this region is given by

$$W = 2\rho c S_m \overline{\langle v_m^2 \rangle} \sigma_m, \tag{45}$$

where $\sigma_m = 4f^2 S_m/c^2$ is the radiation efficiency of a monopole with the velocity distribution of a simply supported plate (Eq. (25)). $S_m = a\lambda_y/4$ is the area of each monopole, and $\overline{\langle v_m^2 \rangle}$ is the

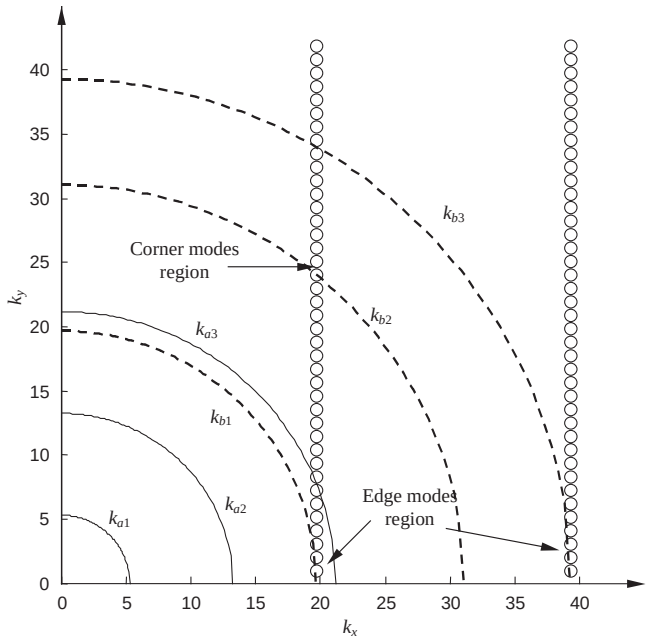

Fig. 18. Comparison of acoustical and structural wavenumber showing the characteristic of the modal radiation of the strip for frequencies between the fundamental and second cut-on natural frequencies. ○, Wavenumber at structural modes; —, acoustic wavenumber at three frequencies; – –, structural wavenumber at corresponding frequencies.

mean square velocity within these monopole regions. The radiation efficiency of the whole strip with light damping can thus be given by

$$\sigma_{0s} = \frac{W}{\rho c a b \overline{\langle v^2 \rangle}} = \frac{2\sigma_m S_m}{ab} = \frac{8 S_m^2 f^2}{abc^2} \tag{46}$$

since $\langle \overline{v_m^2} \rangle = \langle \overline{v^2} \rangle$. Substituting $\lambda_y = 2b/n$, Eq. (46) becomes

$$\sigma_{0s} = \frac{2abf^2}{c^2 n^2} \quad \text{for } f_{1,1} < f < f_{2,1}, \;\; k_y > k_a, \tag{47}$$

where n is the index of modes in the y direction, i.e., along the length.

Eq. (47) will not be appropriate for a very small value of γ. For those cases, the 'corner' modes will not appear and only 'edge' modes will dominate this frequency range. This can be seen from the radiation efficiency of the strip $0.08 \times 3 \times 0.003$ m, as shown in Fig. 14. The absence of 'corner' modes occur if

$$\gamma \leqslant \frac{2\pi}{bc}\left(\frac{B}{\rho h}\right)^{1/2}. \tag{48}$$

For the current case, a strip with $b = 3$ m, this limiting value of γ is 0.0287.

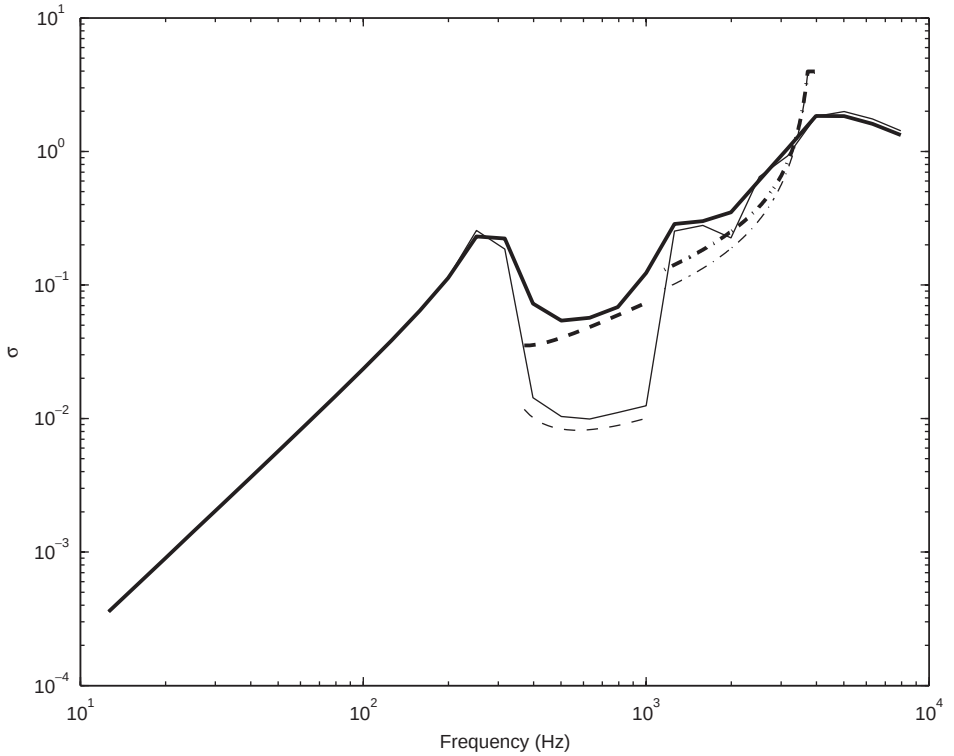

Fig. 19. Estimation of the radiation efficiency of the strip 0.16×3 m. —, Modal summation with $\eta = 0.0005$; thick line; modal summation with $\eta = 0.1$; – –, $\eta = 0.0005$ by Eq. (50); ▬, $\eta = 0.1$ by Eq. (50); ·—·, $\eta = 0.0005$ by Eq. (27); ··—·, $\eta = 0.1$ by Eq. (27).

The characteristics of the nearfield radiation also appear to be different from the case of moderate aspect ratio. The radiation efficiency at 630 Hz for different values of the damping loss factor was presented in Fig. 16 for plates with large and moderate aspect ratios. It is found for the strip that the dependence of the radiation efficiency on the damping loss factor is approximately twice that for the rectangular plate. So the nearfield radiation efficiency for the strip in this region can be approximated as

$$\sigma_{ns} = \frac{8}{\pi}\frac{f}{f_c}\eta \quad \text{for } f_{1,1} < f < f_{2,1}, \;\; k_y > k_a. \tag{49}$$

Combining these two expressions, the radiation efficiency of the damped strip in this region is therefore approximately given by

$$\sigma = \sigma_{0s} + \sigma_{ns} \approx \frac{2abf^2}{c^2 n^2} + \frac{8}{\pi}\frac{f}{f_c}\eta \quad \text{for } f_{1,1} < f < f_{2,1}, \;\; k_y > k_a. \tag{50}$$

Results calculated using Eq. (50) are compared with the results from the modal summation. Fig. 19 shows the results for the strip of dimensions 0.16×3.0 m with values of damping loss

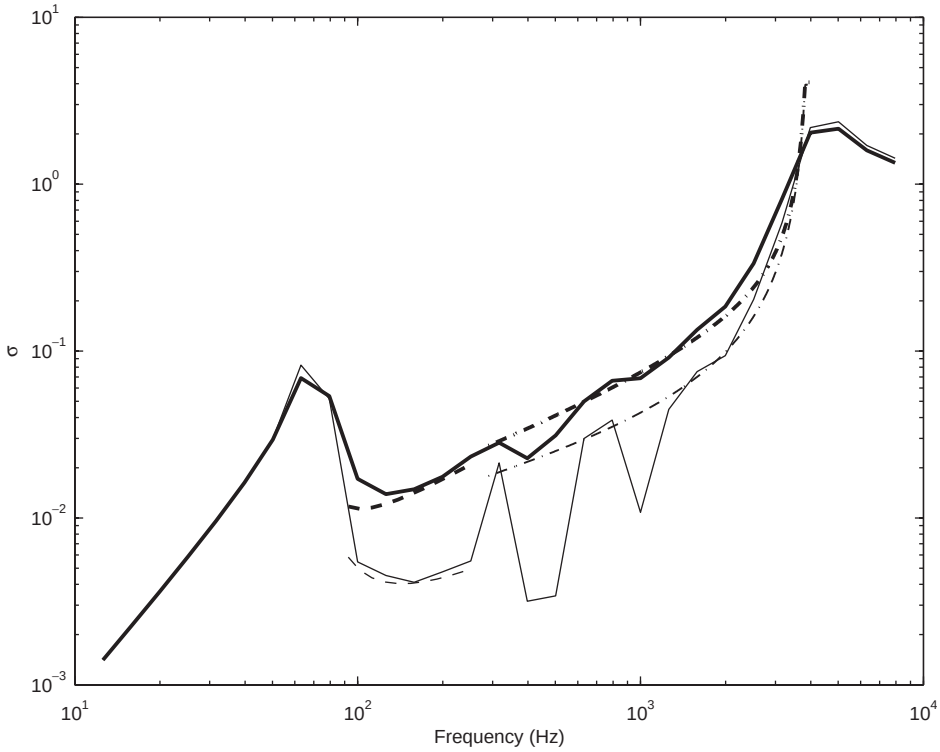

Fig. 20. Estimation of the radiation efficiency of the strip 0.32×3 m. —, Modal summation with $\eta = 0.0005$; thick line, modal summation with $\eta = 0.1$; – –, $\eta = 0.0005$ by Eq. (50); ▬▬, $\eta = 0.1$ by Eq. (50); · — ·, $\eta = 0.0005$ by Eq. (27); ·▬·, $\eta = 0.1$ by Eq. (27).

factor of 0.0005 and 0.1. Although small differences exist, Eq. (50) gives a fairly good approximation for this region. For the strip of dimensions 0.32×3.0 m, the comparison is presented in Fig. 20. The model represented by Eq. (50) is also shown to be a good approximation for the radiation efficiency in this region, in this case 100–250 Hz.

4.4. Summary of approximation formulae for strips

For a rectangular plate with a large aspect ratio (γ smaller than 0.1), Eq. (44) can be used to replace the corresponding part of Eq. (25) for frequencies below the fundamental natural frequency. For frequencies between the fundamental natural frequency and the second cut-on frequency, the radiation efficiency of the strip can be estimated by using Eq. (50). For frequencies between the second cut-on frequency and the critical frequency, the radiation efficiency of the strip can also be approximated with the third expression in Eq. (25) since the mode distribution in this region becomes more evenly spaced the wavenumber domain. This is seen from the comparisons given in Figs. 19 and 20. For frequencies around the critical frequency the results discussed in Section 3.4 apply while above the critical frequency the conventional results of

Eq. (25) remain valid. All these formulae are combined as below

$$\sigma \approx \begin{cases} \dfrac{8.5}{c^2} a^2 f^2 & \text{for } f < f_{1,1} \\ \dfrac{2abf^2}{c^2 n^2} + \dfrac{8}{\pi} \dfrac{f}{f_c} \eta & \text{for } f_{1,1} < f < f_{2,1},\ \ k_y > k_a \text{ and } \dfrac{2\pi}{bc}\left(\dfrac{B}{\rho h}\right)^{1/2} \leqslant \gamma \leqslant 0.1 \\ \dfrac{Pc}{4\pi^2 S f_c} \times \dfrac{(1-\alpha^2)\ln\left(\dfrac{1+\alpha}{1-\alpha}\right) + 2\alpha}{(1-\alpha^2)^{3/2}} + \dfrac{4}{\pi} \dfrac{f}{f_c} \eta & \text{for } f_{2,1} < f < f_c,\ \ \alpha = \sqrt{\dfrac{f}{f_c}} \\ \sigma_c \approx \begin{cases} 1.2 - 1.3 & \text{for } k_c a \leqslant 3 \\ (k_c a)^{1/4} & \text{for } k_c a > 3 \end{cases} & \text{for } f = f_c \\ \left(1 - \dfrac{f_c}{f}\right)^{-1/2} & \text{for } f > f_c. \end{cases} \tag{51}$$

5. Conclusions

The radiation efficiency of plates has been investigated by using the modal summation approach. The radiation efficiency is calculated by considering the average over all possible point force excitation positions. Cross-modal terms do not arise in this averaged radiation efficiency. This averaged radiation efficiency shows the limitations of previous formulae by Maidanik [2] for a strip, a plate with a large aspect ratio. It has been shown that its radiation efficiency below the fundamental frequency is proportional to the square of the shortest edge length rather than the area of the plate. For frequencies between the fundamental natural frequency and the cut-on of modes involving a whole wavelength deformation across the strip, the radiation from the strip can be considered to be equivalent to the radiation of two monopoles each of size $a \times \lambda_y/4$ where λ_y is the wavelength along the length of the strip. The nearfield radiation from the forcing point in this frequency region is proportional to the damping loss factor. It is found that the dependence on the damping loss factor of the nearfield radiation efficiency for the strip is approximately twice that for the rectangular plate with moderate aspect ratio. Finally, an approximate model for calculating the radiation efficiency of a strip has been presented.

Based on the results from the modal summation approach, it is found that the maximum average radiation efficiency expressed in one-third octave bands increases in proportion to $(k_c a)^{1/4}$ for $k_c a > 3$, not $(k_c a)^{1/2}$ as given by Leppington and Maidanik, where k_c is the wavenumber at the critical frequency and a is the shorter edge of the plate. For $k_c a < 3$, the maximum radiation efficiency tends to a constant value between 1.2 and 1.3, depending on the aspect ratio.

References

[1] L. Rayleigh, *The Theory of Sound*, 2nd Edition, 1896 (reprinted by Dover, New York, 1945).

[2] G. Maidanik, Response of ribbed panels to reverberant acoustic fields, *Journal of the Acoustical Society of America* 34 (1962) 809–826.
[3] C.E. Wallace, Radiation resistance of a rectangular panel, *Journal of the Acoustical Society of America* 51 (1972) 946–952.
[4] M.C. Gomperts, Radiation from rigid baffled rectangular plates with general boundary conditions, *Acustica* 30 (1974) 320–327.
[5] M.C. Gomperts, Sound radiation from baffled, thin, rectangular plates, *Acustica* 37 (1977) 93–102.
[6] M. Heckl, Radiation from plane sound sources, *Acustica* 37 (1977) 155–166.
[7] F.G. Leppington, E.G. Broadbent, K.H. Heron, The acoustic radiation efficiency of rectangular panels, *Proceedings of the Royal Society London A* 382 (1982) 245–271.
[8] E.G. Williams, A series expansion of the acoustic power radiated from planar sources, *Journal of the Acoustical Society of America* 73 (1983) 1520–1524.
[9] W.L. Li, An analytical solution for the self- and mutual radiation resistances of a rectangular plate, *Journal of Sound and Vibration* 245 (1) (2001) 1–16.
[10] I.L. Ver, C.I. Holmer, in: L.L. Beranek (Ed.), *Noise and Vibration Control*, McGraw-Hill, New York, 1971, pp. 287–296.
[11] S. Snyder, N. Tanaka, Calculating total acoustic power output using modal radiation efficiencies, *Journal of the Acoustical Society of America* 97 (1995) 1702–1709.
[12] W.L. Li, H.J. Gibeling, Determination of the mutual radiation resistances of a rectangular plate and their impact on the radiated sound power, *Journal of Sound and Vibration* 229 (1999) 1213–1233.
[13] W.L. Li, H.J. Gibeling, Acoustic radiation from a rectangular plate reinforced by finite springs at arbitrary locations, *Journal of Sound and Vibration* 220 (1999) 117–133.
[14] K. Sakagami, K. Michishita, M. Morimoto, Y. Kitamura, Sound radiation from a baffled elastic plate strip of infinite length with various concentrated excitation forces, *Applied Acoustics* 55 (1998) 181–202.
[15] K. Michishita, K. Sakagami, M. Morimoto, U.P. Svensson, Sound radiation from an unbaffled elastic plate strip of infinite length, *Applied Acoustics* 61 (2000) 45–63.
[16] L. Cremer, M. Heckl, E.E. Ungar, *Structure-borne Sound*, 2nd Edition, Springer, Berlin, 1988.
[17] F.J. Fahy, *Sound and Structural Vibration*: *Radiation, Transmission and Response*, Academic Press, London, 1985.